

Vibropolaritonic Reaction Rates in the Collective Strong Coupling Regime: Pollak-Grabert-Hänggi Theory

Matthew Du,^{*} Yong Rui Poh,^{*} and Joel Yuen-Zhou[†]

Department of Chemistry and Biochemistry, University of California San Diego, La Jolla, California 92093, USA

(Dated: January 6, 2023)

Following experimental evidence that vibrational polaritons, formed from collective vibrational strong coupling (VSC) in optical microcavities, can modify ground-state reaction rates, a spate of theoretical explanations relying on cavity-induced frictions has been proposed through the Pollak-Grabert-Hänggi (PGH) theory, which goes beyond transition state theory (TST). However, by considering only a single reacting molecule coupled to light, these works do not capture the ensemble effects present in experiments. Moreover, the relevant light-matter coupling should have been \sqrt{N} times smaller than those used by preceding works, where $N \approx 10^6 - 10^{12}$ is the ensemble size. In this work, we explain why this distinction is significant and can nullify effects from these cavity-induced frictions. By analytically extending the cavity PGH model to realistic values of N , we show how this model succumbs to the polariton “large N problem”, that is, the situation whereby the single reacting molecule feels only a tiny $1/N$ part of the collective light-matter interaction intensity, where N is large.

INTRODUCTION

Vibrational strong coupling (VSC) occurs when molecular vibrational modes interact strongly with infrared photon modes, typically confined in an optical cavity, thus forming new light-matter hybrid modes known as vibrational polaritons [1, 2]. With microcavities such as Fabry-Pérot cavities, these interactions are only appreciable in the presence of a macroscopic number of molecules, that is, VSC is a collective effect [3, 4]. Over the past decade, vibrational polaritons formed from microcavities have been experimentally shown to influence (1) ground-state chemical reactivities [5–12] and (2) vibrational energy transfer processes [13–16], creating a field known as vibropolaritonic chemistry. These experiments, conducted under the following conditions: [17]

- C1. $N \approx 10^6 - 10^{12}$ molecules *collectively* coupled to the cavity,
- C2. in the absence of optical pumping, that is, the reaction relies purely on *thermal fluctuations*,

reported the following observations:

- O1. The cavity may either *enhance* or *suppress* reaction rates;
- O2. Rate modification by the cavity is optimum when the cavity mode is *resonant* with the reactant, spectator and/or solvent vibrational modes, and
- O3. occurs only for the cavity mode at normal incidence ($k = 0$).

Unfortunately, there remains a dearth of theoretical models that successfully explain all five features. In particular, the first class of transitions has, in the absence of VSC, been well-explained by thermal adiabatic rate models [18] such as transition state theory (TST). Along this vein, pioneering studies have attempted to incorporate VSC effects into a classical TST model [3, 19], only to find that the activation energy remains unchanged once the often-neglected dipole self-energy term of the photon mode is included [20] (although this conclusion has been contested by models that account for vibrational quantum effects [21]). The transmission prefactor may, however, be reduced by VSC [20] through a dynamical caging effect similar to the Grote-Hynes theory [22], yet this result fails to account for the collective, resonance and $k = 0$ features present in experiments (i.e. features C1, O2 and O3). This sparked a series of works that considered additional effects such as anharmonicities [23–26], multiple cavity modes [27, 28], inter-mode energy redistributions [29–32], and disorders [33, 34]. A summary of these theoretical results will be presented in an upcoming perspective [35]. Note that considerable efforts have also been devoted to the second class of transitions [36–42] and will not be discussed here.

This paper joins the wave of some recent works [43–45] that explored the possibility of cavity-induced frictions. Through classical trajectory-based simulations over a range of bath frictions, Sun and Vendrell reported cavity-mediated rate enhancements in the low-friction regime that peak when the reacting vibrational mode is resonant with the cavity mode [43] (thereby fulfilling observation O2). Their result is consistent with the Pollak-Grabert-Hänggi (PGH) description [46], an analytical adiabatic rate model that also considers weak energy exchange between the system and bath modes. Here, system refers to a reactive mode, so stronger system-bath couplings (also known as frictions) allow the reacting system to more easily acquire energy from the bath to cross the barrier, thereby accelerating the reaction. Note that the PGH theory is a non-Markovian generalisation of the Kramers turnover model, first pre-

^{*} Both authors contributed equally to this work.

[†] joelyuen@ucsd.edu

dicted by Kramers [47] and later solved by Mel'nikov and Meshkov [48]. Importantly, PGH theory goes beyond TST and is unlike the Grote-Hynes theory [22], which may be reduced to TST [49]. In the context of VSC, Lindoy et al. interpreted the cavity mode as an effective bath mode, which exerts cavity-induced friction on the system [44]. As such, the cavity accelerates chemical reactions when its coupling to the reactive mode is stronger than that of the molecule's inherent bath modes. In both aforementioned works [43, 44], the cavity was assumed to have a single photon mode. Later, Philbin et al. extended the model to an imperfect cavity with multiple confined modes [45] and made qualitatively similar observations apart from sharper resonances and weaker cavity effects.

These studies, while enlightening, were investigated for a single (or few) molecule(s) interacting with light and are therefore not fully representative of the ensemble effects observed in VSC involving microcavities [5–12] (see condition C1). In addition, their numerical results were reported using experimental values of light-matter interactions belonging to an entire molecular ensemble, even though the single-molecule interaction would have been more accurate. This distinction is highly non-trivial: the appropriate single-molecule light-matter coupling g is \sqrt{N} times smaller than the experimentally-measured collective coupling $g\sqrt{N}$, where N is the number of confined molecules estimated to be $\approx 10^6 - 10^{12}$ [50, 51]. Clearly $g \neq g\sqrt{N}$. To demonstrate how collectivity changes the effects of cavity-induced frictions, we analytically extend the PGH model to include a macroscopic number of molecules N , each of which interacts with a single cavity mode [Fig. (1)]. Using a $g\sqrt{N}$ value representative of experimental data, we find that the purported cavity-mediated rate enhancements quickly and expectedly vanish with increasing N and are negligible for realistic values of $N > 20$. In particular, cavity-induced frictions depend on g to leading order in $g\sqrt{N} - 1$, a result familiar to the community of collective VSC [21, 41, 52]. Therefore, for a constant $g\sqrt{N} - 1 \approx g\sqrt{N}$, we find that g and thus cavity-mediated frictions diminish with realistic values of N . This is a reminder of the polariton “large N problem” [4], that is, that any benefit from the polaritons is often lost to the penalty of having a large number ($N - 1$) of non-reacting molecules compete with a single reacting molecule for the cavity [Fig. (2)]. Finally, we qualitatively argue why our observations remain valid even with disorder and multiple cavity modes.

With reference to the five features described earlier, our model fully addresses C1, C2 and O2 and partially addresses O1 by dealing only with rate enhancements. Note that the collective effect described by condition C1 is the novel part of this work.

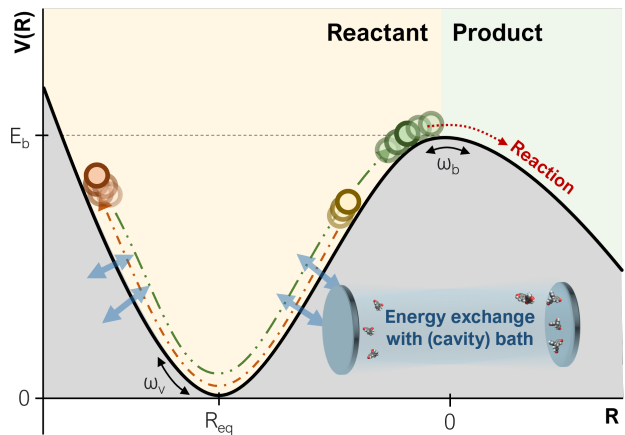


FIG. 1. PGH theory and its application to VSC. The PGH particle moves classically along a “system” reactive mode (coordinate R) coupled to a thermal bath. The potential along the reactive mode has a barrier E_b (position $R = 0$, harmonic frequency ω_b), which separates a potential well (equilibrium position $R = R_{eq}$, harmonic frequency ω_v) from the continuum; these two regions signify the reactant and product regions respectively. The particle starts off with energy $E < E_b$ (yellow particle) and is unable to cross the barrier. Instead, it moves to and fro between the barrier and the reactant region (red and green paths), during which it exchanges energy with the thermal bath through the system-bath couplings (or frictions). These couplings are small so the particle may, at some point (green particle), acquire sufficient energy from the thermal bath to cross the barrier ($E \geq E_b$) and react. PGH theory estimates the rate of this process – effectively, it computes the rate of thermally-activated chemical reactions in the low bath friction limit. When applied to VSC, the potential is the adiabatic electronic ground-state potential energy surface. In the single-molecule regime, the cavity mode serves as an effective bath mode [44] whereas, in the collective regime, the cavity and additional $N - 1$ non-reactive vibrational modes couple to form two polariton modes, which then become effective bath modes.

RESULTS AND DISCUSSIONS

Outside the cavity, the PGH model [46] considers a single reactive (system) mode of coordinate R coupled to a harmonic thermal bath of coordinates $\{Q_\alpha\}$ and frequencies $\{\omega_\alpha\}$. The potential of the reactive mode has a barrier of height E_b separating a well from the continuum [Fig. (1)]. A particle (such as a single molecule) moves along its reactive and bath modes classically; it starts from a metastable state in the well and, through energy exchange with the thermal bath modes, harnesses sufficient energy to cross the barrier, signifying a reaction of which the rate may be computed. Working in mass-weighted coordinates, the Hamiltonian for this model is

$$H_{\text{PGH}} = \frac{\dot{R}^2}{2} + V(R) + \sum_{\alpha=1}^N \left[\frac{\dot{Q}_\alpha^2}{2} + \frac{1}{2} (\omega_\alpha Q_\alpha + \gamma_\alpha R)^2 \right], \quad (1)$$

where $\{\gamma_\alpha \in \mathbb{R}\}$ are the system-bath couplings (or frictions), and $V(R)$ is the potential along the reactive coordinate R and is modelled harmonically near the barrier and well bottom (with imaginary frequency $i\omega_b$ and real frequency ω_v respectively; $\omega_b, \omega_v \in \mathbb{R}^+$). It is convenient to work in the normal mode basis around the barrier region, which comprises one unstable mode u of imaginary frequency $i\Omega_b$ ($\Omega_b \in \mathbb{R}^+$) and \mathcal{N} stable modes $\{s_k\}$ of real frequencies $\{\Omega_k \in \mathbb{R}^+\}$. This implies that (1) the reaction occurs along the unstable mode since it has a barrier (of frequency Ω_b), and (2) in the weak system-bath coupling limit, the reactive mode is composed mostly of the unstable mode such that contributions from the stable modes may be used to characterise these system-bath couplings. Mathematically, if we define $R = Q_1 = \dots = Q_{\mathcal{N}} = 0$ when the particle is at the barrier and expand R in the stable-unstable mode basis as

$$R = c_{00}u + \sum_{k=1}^{\mathcal{N}} c_{0k}s_k \quad (2)$$

with $c_{0k} \in \mathbb{R}$ for all $k = 0, 1, \dots, \mathcal{N}$ and $\sum_{k=0}^{\mathcal{N}} c_{0k}^2 = 1$, then the total system-bath coupling may be characterised by

$$\epsilon = \sum_{k=1}^{\mathcal{N}} \frac{c_{0k}^2}{c_{00}^2} = \frac{1}{c_{00}^2} - 1. \quad (3)$$

PGH theory focuses on the weak system-bath coupling limit ($\epsilon \ll 1$), so we expect larger ϵ to improve energy exchange between system and bath modes and therefore increase the reaction rate. Finally, by analysing the energy flow between the stable and unstable modes during the particle's path in the well (during which the stable and unstable modes are no longer normal modes), the reaction rate is predicted to be [46]

$$k = \kappa k_{1\text{DTST}}, \quad (4)$$

where $k_{1\text{DTST}} = \frac{\omega_v}{2\pi} e^{-\beta E_b}$ is the rate calculated using 1D transition state theory (1D-TST) and is independent of system-bath couplings, and

$$\kappa = \frac{\Omega_b}{\omega_b} \times \exp \left[\frac{1}{\pi} \int_{-\infty}^{\infty} \frac{dy}{1+y^2} \ln \left(1 - e^{-(\beta \Delta E) \frac{1+y^2}{4}} \right) \right] \quad (5)$$

is the transmission factor due to system-bath couplings and serves as a proxy measure of the bath's effects on the reaction rate. Here, $\beta = (k_B T)^{-1}$, with T as temperature. Also, ΔE characterises the system-bath energy exchange and has the form

$$\Delta E = \frac{1}{2} \sum_{k=1}^{\mathcal{N}} \frac{c_{0k}^2}{c_{00}^2} \left| \tilde{F}(\Omega_k) \right|^2, \quad (6)$$

where $\tilde{F}(\Omega_k)$ is the Fourier transform of the effective force experienced by the unstable mode. The latter may be solved analytically for a piecewise differentiable

parabolic potential of the form

$$V(R) = \begin{cases} \frac{1}{2} \omega_v^2 (R - R_{\text{eq}})^2 & R \leq R', \\ -\frac{1}{2} \omega_b^2 R^2 + E_b & R > R', \end{cases} \quad (7)$$

where $R_{\text{eq}} = -\sqrt{2E_b(1/\omega_v^2 + 1/\omega_b^2)}$ and $R' = R_{\text{eq}}\omega_v/(\omega_v^2 + \omega_b^2)$ are derived from making both $V(R)$ and $\partial_R V(R)$ continuous at $R = R'$ (thus giving two conditions that solve for two unknowns). The result is

$$\left| \tilde{F}(\Omega_k) \right|^2 = \frac{4(R'/c_{00})^2 \Omega_b^2 (\omega_{\text{eff}}^2 + \Omega_b^2)^2}{\Omega_k^2 (\Omega_k^2 - \omega_{\text{eff}}^2)^2} \times [\Omega_b \sin(\Omega_k \tau/2) + \Omega_k \cos(\Omega_k \tau/2)]^2, \quad (8)$$

where $\omega_{\text{eff}} = \sqrt{c_{00}^2 (\omega_v^2 + \omega_b^2) - \Omega_b^2}$ is the effective well frequency experienced by the unstable mode, and τ is the system-bath interaction time obtained by solving the coupled equations

$$\begin{cases} \cos \omega_{\text{eff}} \tau = (\Omega_b^2 - \omega_{\text{eff}}^2) / (\Omega_b^2 + \omega_{\text{eff}}^2), \\ \sin \omega_{\text{eff}} \tau = -(2\Omega_b \omega_{\text{eff}}) / (\Omega_b^2 + \omega_{\text{eff}}^2). \end{cases}$$

Focusing on Eqs. (4), (5) and (6), we find that stronger system-bath couplings, characterised by $\epsilon = \sum_{k=1}^{\mathcal{N}} c_{0k}^2/c_{00}^2$, facilitate energy exchange ΔE between the modes and also modify the unstable mode barrier frequency Ω_b . While the former increases κ , the reaction rate relative to that from 1D-TST, the latter may change κ in either directions.

To apply PGH theory to VSC, Lindoy et al. considered the reactive mode (with finite barrier like Eq. (7)) to be bilinearly coupled to both the harmonic molecular bath and a single cavity mode [44]. This bilinear light-matter interaction originates from the Pauli-Fierz non-relativistic QED Hamiltonian [53–55] and may be interpreted as a cavity-induced friction in the PGH framework (i.e. the cavity mode acts as an effective bath mode). Since the reactive mode belongs to a single reacting molecule, its harmonic molecular bath corresponds to its “solvent” environment. Chemical reactions are rare events, and it is unlikely for two molecules to react simultaneously. As such, to extend this model to the collective regime, we need to include $N - 1$ other non-reacting molecules, each with its own harmonic (and, therefore, non-reactive) vibrational mode also coupled bilinearly to the *same* cavity mode and its own *separate* harmonic molecular bath. (Alternatively, this model may be interpreted as explicitly describing the set-up of “cooperative VSC”, whereby a small amount of reactive species is placed in a sea of chemically inert molecules, all of which couple to the cavity in the same fashion [6, 10, 11, 56].)

In the following paragraphs, we will show that, through a normal mode transformation, we may rewrite the subsystem comprising the cavity and $N - 1$ non-reactive molecules into a pair of polariton modes bilinearly coupled to the reactive mode. Just like the single-molecule models [43–45], these bilinear couplings represent cavity-induced frictions, which accelerate the reaction in the low-friction regime.

The Hamiltonian describing the above model is, in mass-weighted coordinates,

$$H = T_r + V_r(R) + H_{\text{nr-c}} + H_{\text{r-c}} + H_{\text{bath}}, \quad (9)$$

where $T_r = \dot{R}^2/2$ is the kinetic energy of the reactive mode with coordinate R , $V_r(R)$ is the piecewise differentiable parabolic potential of the reactive mode as described by Eq. (7) (well frequency ω_v , barrier frequency ω_b),

$$H_{\text{nr-c}} = \sum_{j=1}^{N-1} \left(\frac{\dot{X}_j^2}{2} + \frac{\omega_v^2}{2} X_j^2 \right) + \frac{q_c^2}{2} + \frac{1}{2} \left(\omega_c q_c + 2g \sum_{j=1}^{N-1} X_j \right)^2 \quad (10)$$

represents the couplings between the cavity mode (coordinate q_c , frequency ω_c) and $N - 1$ non-reactive vibrational modes (coordinates $\{X_j\}$, frequency ω_v), as well as their kinetic and potential energies,

$$H_{\text{r-c}} = \left(\omega_c q_c + 2g \sum_{j=1}^{N-1} X_j \right) 2gR + 2g^2 R^2 \quad (11)$$

represents the couplings between the reactive mode and the subsystem of cavity and $N - 1$ non-reactive vibrational modes, and H_{bath} represents all N sets of molecular bath modes that belong to the single reactive and $N - 1$ non-reactive vibrational modes. As mentioned earlier, this Hamiltonian may be derived from the cavity QED Hamiltonian in the dipole gauge, under the cavity Born-Oppenheimer approximation, after assuming all molecules to be in the adiabatic electronic ground state [53–55]; more details may be found in Ref. [20]. Here, we consider only a single cavity mode and assume that all $N - 1$ non-reactive vibrational modes have the same spatial alignments and frequencies ω_v as the potential well of the reactive mode (the result remains qualitatively unchanged under isotropic alignment of dipoles and will be explained later). As such, all molecules couple equally to the cavity mode, each with the same coupling amplitude of $g = -\boldsymbol{\mu}'_0 \cdot \boldsymbol{\epsilon} / \sqrt{4\epsilon_0 \mathcal{V}}$, where $\boldsymbol{\epsilon}$ is the polarisation unit vector of the cavity mode, \mathcal{V} is the cavity's effective quantisation volume, and $\boldsymbol{\mu}'_0$ is the linear change of the dipole moment along each vibrational mode near its equilibrium position (well bottom for the reactive mode), identical for all modes (i.e. $\boldsymbol{\mu}'_j = \boldsymbol{\mu}'_r = \boldsymbol{\mu}'_0$ for all $j = 1, \dots, N - 1$). While $H_{\text{nr-c}} + H_{\text{r-c}}$ [Eqs. (10) and (11)], which describe couplings to the reactive mode, is not yet in the form of H_{PGH} [Eq. (1)], a normal mode transformation will do the trick. Exploiting the symmetries created by the assumptions above, we can rewrite the $N - 1$ degenerate non-reactive vibrational modes into a single bright mode with coordinate

$$Q_B = \frac{1}{\sqrt{N-1}} \sum_{j=1}^{N-1} X_j \quad (12)$$

and $N - 2$ dark modes with coordinates

$$Q_\zeta = \frac{1}{\sqrt{N-1}} \sum_{j=1}^{N-1} A_{j,\zeta} X_j, \quad \zeta = 2, \dots, N-1,$$

where the coefficients $\{A_{j,\zeta}\}$ are real-valued for all j and ζ and satisfy the orthonormality conditions of

$$\sum_{j=1}^{N-1} A_{j,\zeta} = 0 \quad \text{and} \quad \sum_{j=1}^{N-1} \frac{A_{j,\zeta} A_{j,\eta}}{N-1} = \delta_{\zeta\eta},$$

with $\delta_{\zeta\eta}$ representing the Kronecker delta. Then, $H_{\text{nr-c}}$ [Eq. (10)] becomes

$$H_{\text{nr-c}} = \sum_{\zeta=2}^{N-1} \left(\frac{\dot{Q}_\zeta^2}{2} + \frac{\omega_v^2}{2} Q_\zeta^2 \right) + \frac{\dot{Q}_B^2}{2} + \frac{\omega_v^2}{2} Q_B^2 + \frac{q_c^2}{2} + \frac{1}{2} \left(\omega_c q_c + 2g\sqrt{N-1} Q_B \right)^2, \quad (13)$$

i.e. only the bright mode has the correct symmetry to couple with the cavity. Performing a normal mode transformation on these two modes gives two polariton modes with coordinates Q_\pm and frequencies ω_\pm (see Appendix 1). By expressing $H_{\text{nr-c}}$ [Eq. (13)] and $H_{\text{r-c}}$ [Eq. (11)] in terms of the polariton modes, the Hamiltonian becomes

$$H = H_{\text{eff}} + H_{\text{bath}} + \sum_{\zeta=2}^{N-1} \left(\frac{\dot{Q}_\zeta^2}{2} + \frac{\omega_v^2}{2} Q_\zeta^2 \right), \quad (14)$$

where

$$H_{\text{eff}} = \frac{\dot{R}^2}{2} + V_r(R) + \sum_{\alpha=\pm} \left[\frac{\dot{Q}_\alpha^2}{2} + \frac{1}{2} (\omega_\alpha Q_\alpha + 2g_\alpha R)^2 \right], \quad (15)$$

such that the subsystem of cavity and $N - 1$ non-reactive vibrational modes forms a pair of effective polariton bath modes (coordinates Q_\pm) that interact with the reactive mode through couplings g_\pm . These system-polariton couplings g_\pm are analogous to the cavity-induced friction g described by single-molecule models [43–45] (for instance, compare Eq. (15) with Eq. (3) of Ref. [44], which denotes g by $\eta_c \sqrt{\omega_c/2}$). Note that the dark modes (coordinates Q_2, \dots, Q_{N-1}) do not couple to the reactive mode and may be neglected in our future analysis.

The Hamiltonian [Eq. (14)] is now in the form of Eq. (1) and the PGH results may be directly applied. In principle, H_{bath} should comprise molecular bath modes interacting with the polariton and reactive modes through bilinear couplings drawn from a spectral density. However, single-molecule analyses of this system suggest that the cavity has the strongest effect when the molecular bath modes are weakly coupled to the reactive mode, such that the cavity's coupling is the most prominent among all the effective bath modes [44, 45]. We expect similar results in the presence of $N - 1$ non-reacting molecules and thus consider the zero

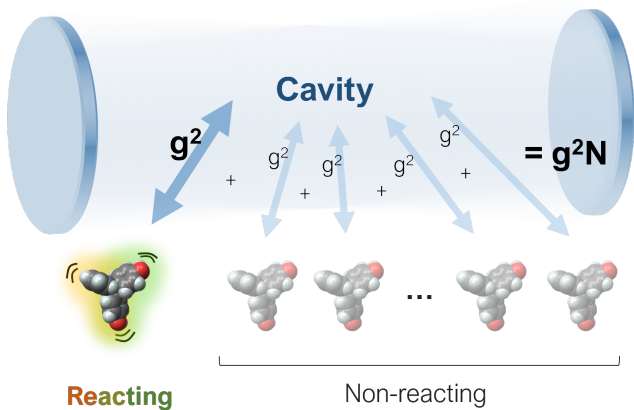


FIG. 2. Hierarchy of interactions with the reacting molecule. The cavity couples collectively to all N molecules with intensity $g^2 N$, so each molecule experiences an average coupling intensity of g^2 . From the reacting molecule's perspective, it first couples directly and most strongly to the cavity with intensity g^2 . The same molecule also couples to the remaining $N - 1$ non-reacting molecules, but only through the cavity, thus making this a second-order process with intensities proportional to the product of the two sub-processes' couplings: g^2 and $g^2 (N - 1)$. This effect is captured in the series expansion of system-polariton couplings g_{\pm} [Eq. (16)] and is an important part of the polariton “large N problem”.

bath friction limit, i.e. we set $H_{\text{bath}} = 0$ and focus on H_{eff} [Eq. (15)]. This simplification will not change the qualitative outcome. Before we present our numerical results, we expand, in orders of $g\sqrt{N-1}$, the system-polariton couplings g_{\pm} (i.e. cavity-induced frictions), the total system-polariton coupling ϵ and the unstable mode barrier frequency Ω_b , all of which characterise the cavity's effects on the reaction rate. In the zero-detuning limit of $\omega_c \approx \omega_v$, we get

$$g_{\pm} = \frac{g}{\sqrt{2}} \pm \frac{g^2 \sqrt{N-1}}{2\sqrt{2}\omega_v} + \mathcal{O}(g^3(N-1)), \quad (16)$$

$$\epsilon = \frac{4\omega_v^2 g^2}{(\omega_v^2 + \omega_b^2)^2} + \mathcal{O}(g^4(N-1)), \quad (17)$$

$$\text{and } \Omega_b = \omega_b - \frac{2\omega_b g^2}{\omega_v^2 + \omega_b^2} + \mathcal{O}(g^4(N-1)) \quad (18)$$

(see Appendix 2, which uses Ref. [57]). The first term in g_{\pm} represents the single-molecule light-matter coupling g , a first-order process that dominates reaction dynamics and characterises the cavity-induced friction in single-molecule models [44, 45]. The second term represents couplings between the reactive and $N - 1$ non-reactive vibrational modes, a second-order process characterised by $g(g\sqrt{N-1})$. Notice from the expansion coefficients that light-matter coupling enhances the reaction rate through ϵ and retards the reaction rate through Ω_b , observations that concur with the single-molecule analysis [44]. Regardless, to leading order in $g\sqrt{N-1}$, all three parameters depend only on g , the single-molecule coupling, and not on N . For a fixed collective light-matter coupling $g\sqrt{N-1} \approx g\sqrt{N}$ – the experimentally measurable parameter – the cavity's effects (including the friction g_{\pm}) diminish as N grows.

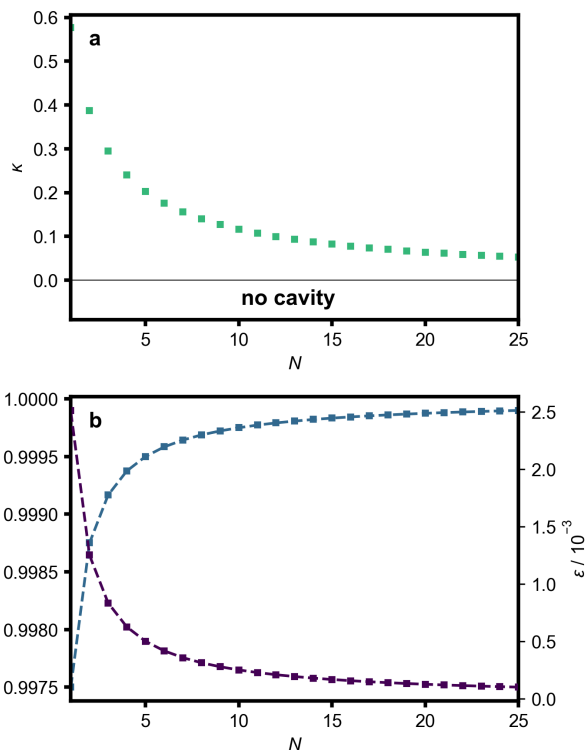


FIG. 3. Cavity effects on the PGH model in the collective regime of $N > 1$. (a) κ , the reaction rate relative to that from 1D-TST, decreases quickly with increasing N . Due to the absence of molecular bath modes in our model, $\kappa \rightarrow 0$ outside the cavity. With realistic values of $N > 20$, we find that $\kappa \rightarrow 0$ too; this suggests that the reaction rate approaches the no-cavity result in the collective regime and cavity effects are lost. (b) Both the unstable mode barrier frequency Ω_b (blue) and the total system-polariton coupling ϵ (purple) approach the no-cavity limit ($\Omega_b/\omega_b \rightarrow 1$ and $\epsilon \rightarrow 0$) with $N > 20$. This is attributable to the tiny single-molecule light-matter coupling g if we were to consider a realistic experimental set-up of $N > 20$ molecules collectively coupled to the cavity (the polariton “large N problem”). Markers represent numerical results while dotted lines represent analytical results obtained from series expansions in $g\sqrt{N-1}$ [Eqs. (17) and (18)]. All plots were generated with the following parameters: equal cavity, vibrational and barrier frequencies $\omega_c = \omega_v = \omega_b$; collective light matter coupling $g\sqrt{N} = 0.05\omega_v$; barrier height $E_b = 20k_B T$.

Such perturbative results have been observed previously [21, 41, 52] and is a reminder of the polariton “large N problem” [4], i.e. cavity effects under VSC are mostly characterised by the single-molecule coupling g , a small parameter due to weak photon confinements in microcavities, and should not be confused with the collective coupling $g\sqrt{N}$, which is much larger and hence experimentally observable [Fig. (2)].

The analytical solutions presented in Eqs. (16), (17) and (18) agree with numerical simulations conducted at $\omega_c = \omega_v = \omega_b$, $g\sqrt{N} = 0.05\omega_v$ and $E_b = 20k_B T$ [Fig. (3)]. More importantly, κ , the reaction rate relative to that from 1D-TST, diminishes rapidly with N and approaches the no-cavity limit after $N > 20$ (experimentally, $N \approx 10^6 - 10^{12}$ [50, 51]). We note that,

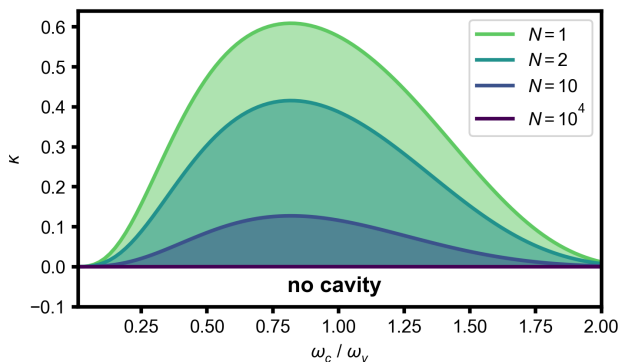


FIG. 4. Effects of cavity detunings on reaction rates. In the single-molecule regime ($N = 1$), VSC enhances the reaction rate with maximum modifications observed at slightly negative detunings ($\omega_c \lesssim \omega_v$). The same trend is observed in the collective regime ($N > 1$), but with decreasing rate enhancements at large N . Note that $\kappa \rightarrow 0$ outside the cavity (see Fig. (3) caption). All plots were generated with the following parameters: collective light matter coupling $g\sqrt{N} = 0.05\omega_v$; barrier height $E_b = 20k_B T$; barrier frequency $\omega_b = \omega_v$.

due to the lack of molecular bath, further removing the cavity (say, $\omega_c \rightarrow 0$ or $g\sqrt{N} \rightarrow 0$) would imply $\kappa \rightarrow 0$ since no effective bath modes are present to provide energy for the PGH particle to cross the barrier (the same conclusion can also be made from Eqs. (5) and (6)). Therefore, any non-zero value of κ must be due to the cavity. Next, across different cavity frequencies ω_c relative to the well vibrational frequency ω_v [Fig. (4)], we find maximum rate enhancements at a value of ω_c slightly below ω_v , a result that agrees with the single-molecule analysis [44] and has been attributed to the non-linearity of $V(R)$ [Eq. (7)]. Again, such rate enhancements disappear quickly with N .

A few comments are now in order:

- We note that, by keeping $g\sqrt{N}$ constant at an experimentally-feasible value, it follows that g must be tiny as $N \rightarrow \infty$. The importance of this work, however, is not what happens when N is infinitely large, but rather what happens when experimental values of N is considered, which happens to be large at $\approx 10^6 - 10^{12}$ [50, 51]. Taking this approach allows us to emphasise the errors incurred by single-molecule models [43–45], which disregard contributions from non-reacting molecules and even treats the light-matter coupling as the collective one (i.e. incorrectly set $g \approx g\sqrt{N}$). From another perspective, since $g\sqrt{N} \approx 10^{-2}\omega_v$, experimental values of g should be estimated as $\approx (10^{-5} - 10^{-8})\omega_v$, a tiny value due to weak photon confinements in microcavities.
- Even if g were to be kept constant at an *appreciable* value (which, *we emphasise*, has only been reported in nanoplasmonic cavities [58, 59] and does *not* coincide with experimental observations of rate enhancements), κ still decreases with in-

creasing N since the growing ensemble reduces the cavity’s catalytic efficiency towards the single reacting molecule. This effect is noteworthy in showing how single-molecule models are not only limited by their choice of g but also the absence of entropic effects from an explicit consideration of the ensemble.

- Note that, unlike Refs. [3, 19], the discussion above remains unchanged if the reactive and $N - 1$ non-reactive vibrational modes have isotropic spatial alignments. In that case, the single-molecule light-matter coupling $g = -\boldsymbol{\mu}'_0 \cdot \boldsymbol{\epsilon} / \sqrt{4\epsilon_0 \mathcal{V}}$ is replaced by a weighted coupling $-\sqrt{\langle \mu_j'^2 \rangle_{N-1}} / \sqrt{4\epsilon_0 \mathcal{V}}$, whereby $\langle \mu_j'^2 \rangle_{N-1} \equiv (N - 1)^{-1} \sum_{j=1}^{N-1} (\boldsymbol{\mu}'_j \cdot \boldsymbol{\epsilon})^2$ reflects the average vibrational mode alignment-*squared* and thus does not vanish in the isotropic limit ($\boldsymbol{\mu}'_j$ is the linear change in the dipole moment of molecule j). Of course, the cavity effects still vanish with realistic values of N .
- Also, given how the studied cavity effects depend on g and not $g\sqrt{N}$ to leading order of the latter term (see Eqs. (16), (17) and (18)), it is unlikely that disorder will significantly affect the reaction rate. Indeed, simulations conducted for $N \leq 3000$ molecules showed little rate modifications due to disorder.
- Interestingly, results from the single molecule model [44] remained qualitatively unchanged when multiple cavity modes were considered, with the exception of sharper cavity resonances and weaker cavity effects [45]. As such, our collective VSC analysis should also hold beyond the single cavity mode limit, provided that the number of molecules per photon mode remains close to the values of N here studied [51, 60].
- Finally, our model and calculations do not show cavity enhancement effects of friction due to spatial delocalisation of eigenstates [42]. We expect these effects to only increase reaction rates by a moderate amount (as discussed in Supplementary Information S2.3 of Ref. [61]). Furthermore, these effects will only arise if there are additional near-field electrostatic interactions among molecules, which have been ignored in this model in light of how weak they are in the vibrational regime.

CONCLUSION

In conclusion, thermal reaction rate models, such as the PGH theory, offer a possible explanation for changes in chemical kinetics within the single-molecule VSC model [43–45]. Unfortunately, this explanation breaks down with collective VSC commonly found in vibropolaritonic chemistry experiments. In this regime, $N \approx 10^6 - 10^{12}$ molecules simultaneously couple to the

cavity [50, 51]. As such, the single reacting molecule experiences only a tiny $1/N$ part of the experimentally-observed light-matter interaction, the remaining of which is shared among the macroscopic number $(N-1)$ of non-reacting molecules, thus negating most rate effects due to the cavity. Overall, there remains little satisfactory explanation for rate modifications observed in vibropolaritonic chemistry experiments and the search continues.

ACKNOWLEDGEMENTS

Acknowledgment is made to the donors of The American Chemical Society Petroleum Research Fund for support of this research through the ACS PRF 60968-ND6 Grant. We also thank Arghadip Koner for helpful discussions.

APPENDIX 1: DERIVING POLARITON MODES FROM THE SUBSYSTEM OF CAVITY AND BRIGHT MODES

Here, we outline the derivation of the polariton modes (coordinates Q_{\pm}) through a normal mode transformation of the cavity mode and bright mode (coordinates q_c and Q_B respectively). As an example, we work in the zero cavity detuning limit ($\omega_c = \omega_v$), but the same principle applies for any general cavity frequency ω_c . Starting from $H_{\text{nr-c}}$ [Eq. (13)] and disregarding the dark modes, we define

$$H_{\text{nr-c}}^{\text{eff}} = H_{\text{nr-c}} - \sum_{\zeta=2}^{N-1} \left(\frac{\dot{Q}_{\zeta}^2}{2} + \frac{\omega_{\zeta}^2}{2} Q_{\zeta}^2 \right) \quad (19)$$

$$= \frac{\dot{Q}_B^2}{2} + \frac{\dot{q}_c^2}{2} + \frac{\omega_v^2}{2} Q_B^2 + \frac{1}{2} \left(\omega_v q_c + 2g\sqrt{N-1} Q_B \right)^2 \quad (20)$$

$$\equiv \frac{\dot{Q}_B^2}{2} + \frac{\dot{q}_c^2}{2} + \frac{1}{2} \sum_{k,l=0,1} x_k \mathcal{H}_{kl} x_l, \quad (21)$$

where $x_0 = q_c$ and $x_1 = Q_B$, and diagonalise the Hessian matrix

$$\mathcal{H} = \begin{pmatrix} \omega_v^2 & 2\omega_v g\sqrt{N-1} \\ 2\omega_v g\sqrt{N-1} & \omega_v^2 + 4g^2(N-1) \end{pmatrix} \quad (22)$$

to get the polariton eigenvalues and (normalised) eigenvectors as

$$\omega_{\pm}^2 = \omega_v^2 + 2g^2(N-1) \pm 2g\sqrt{N-1} \sqrt{g^2(N-1) + \omega_v^2}, \quad (23)$$

$$Q_{\pm} = \left(-\frac{g\sqrt{N-1}}{\omega_v} \pm \sqrt{1 + \frac{g^2(N-1)}{\omega_v^2}} \right) \frac{q_c}{K_{\pm}} + \frac{Q_B}{K_{\pm}}, \quad (24)$$

with normalisation constants

$$K_{\pm} = \sqrt{2 + \frac{2g^2(N-1)}{\omega_v^2} \mp \frac{2g\sqrt{N-1}}{\omega_v} \sqrt{1 + \frac{g^2(N-1)}{\omega_v^2}}}. \quad (25)$$

Note that the eigenvalues of \mathcal{H} give the square of the polariton mode frequencies. Also, we have assumed $g \geq 0$ without loss of generality. We may then write $H_{\text{nr-c}}^{\text{eff}}$ [Eq. (20)] in terms of these polariton normal modes as

$$H_{\text{nr-c}}^{\text{eff}} = \sum_{\alpha=\pm} \left(\frac{\dot{Q}_{\alpha}^2}{2} + \frac{\omega_{\alpha}^2}{2} Q_{\alpha}^2 \right). \quad (26)$$

Next, noting from Eq. (24) that, after (re-)normalisation,

$$q_c = \left(-\frac{g\sqrt{N-1}}{\omega_v} - \sqrt{1 + \frac{g^2(N-1)}{\omega_v^2}} \right) \frac{Q_-}{K_-} + \left(-\frac{g\sqrt{N-1}}{\omega_v} + \sqrt{1 + \frac{g^2(N-1)}{\omega_v^2}} \right) \frac{Q_+}{K_+}, \quad (27)$$

$$Q_B = \frac{Q_-}{K_-} + \frac{Q_+}{K_+}, \quad (28)$$

we write $H_{\text{r-c}}$ [Eq. (11)] in terms of the polariton modes to get

$$H_{\text{r-c}} = \sum_{\alpha=\pm} (2g_{\alpha}\omega_{\alpha}Q_{\alpha}R + 2g_{\alpha}^2R^2), \quad (29)$$

where

$$g_{\pm} = \frac{g}{\omega_{\pm}K_{\pm}} \left(g\sqrt{N-1} \pm \sqrt{\omega_v^2 + g^2(N-1)} \right), \quad (30)$$

are the system-polariton couplings and we have noted that $g_+^2 + g_-^2 = g^2$. Combining Eqs. (9), (19), (26) and (29) and completing the squares give Eqs. (14) and (15).

APPENDIX 2: SERIES EXPANSIONS OF g_{\pm} , ϵ AND Ω_b

Here, we outline the approach taken to expand g_{\pm} , ϵ and Ω_b in orders of $g\sqrt{N-1}$. For simplicity, we set the cavity detuning as zero, i.e. $\omega_c = \omega_v$. Then, g_{\pm} may be expanded directly from Eq. (30) to get Eq. (16). Next, we find the unstable and stable modes by performing a normal mode transformation on the Hamiltonian H_{eff} [Eq. (15)] near the barrier region. Noting that $V(R) \approx -\frac{1}{2}\omega_b^2 R^2 + E_b$ in this region [Eq. (7)], we define

$$H_{\text{eff}}^{(b)} = \frac{\dot{R}}{2} + \sum_{\alpha=\pm} \frac{\dot{Q}_{\alpha}^2}{2} + E_b + \frac{1}{2} \sum_{k,l=0,1,2} y_k K_{kl}^{(b)} y_l, \quad (31)$$

with $y_0 = R$, $y_1 = Q_-$ and $y_2 = Q_+$, and diagonalise the force constant matrix

$$K^{(b)} = \begin{pmatrix} -\omega_b^2 + 4g_-^2 + 4g_+^2 & 2g_- \omega_- & 2g_+ \omega_+ \\ 2g_- \omega_- & \omega_-^2 & 0 \\ 2g_+ \omega_+ & 0 & \omega_+^2 \end{pmatrix} \quad (32)$$

to get an unstable coordinate u with negative eigenvalue $-\Omega_b^2$ ($\Omega_b \in \mathbb{R}^+$) and two stable coordinates $\{s_k\}$ with positive eigenvalues $\{\Omega_k^2\}$ ($\Omega_k \in \mathbb{R}^+$). Since $K^{(b)}$ is an arrowhead matrix, the secular equation and modal matrix (which are used to find the eigenvalues and eigenvectors) have simple forms [57]. In particular, $-\Omega_b^2$ satisfy the following equation

$$\Omega_b^2 = \omega_b^2 \left(1 + \frac{4g_-^2}{\omega_-^2 + \Omega_b^2} + \frac{4g_+^2}{\omega_+^2 + \Omega_b^2} \right)^{-1}, \quad (33)$$

which is solved using perturbation theory in orders of $g\sqrt{N-1}$ to get Eq. (18). Also, c_{00} , the contribution of u to R , can be found from the modal matrix as

$$c_{00} = \left(\sqrt{1 + \left(\frac{2g_- \omega_-}{-\Omega_b^2 - \omega_-^2} \right)^2 + \left(\frac{2g_+ \omega_+}{-\Omega_b^2 - \omega_+^2} \right)^2} \right)^{-1}, \quad (34)$$

which, using Eq. (18) and noting the definition of ϵ in Eq. (3), gives Eq. (17) through a series expansion in $g\sqrt{N-1}$.

-
- [1] J. P. Long and B. S. Simpkins, *ACS Photonics* **2**, 130 (2015).
- [2] A. Shalabney, J. George, J. Hutchison, G. Pupillo, C. Genet, and T. W. Ebbesen, *Nature Communications* **6**, 5981 (2015).
- [3] J. A. Campos-Gonzalez-Angulo and J. Yuen-Zhou, *The Journal of Chemical Physics* **152**, 161101 (2020).
- [4] L. A. Martínez-Martínez, E. Eizner, S. Kéna-Cohen, and J. Yuen-Zhou, *The Journal of Chemical Physics* **151**, 054106 (2019).
- [5] A. Thomas, J. George, A. Shalabney, M. Dryzhakov, S. J. Varma, J. Moran, T. Chervy, X. Zhong, E. Devaux, C. Genet, J. A. Hutchison, and T. W. Ebbesen, *Angewandte Chemie International Edition* **55**, 11462 (2016).
- [6] J. Lather, P. Bhatt, A. Thomas, T. W. Ebbesen, and J. George, *Angewandte Chemie International Edition* **58**, 10635 (2019).
- [7] K. Hirai, R. Takeda, J. A. Hutchison, and H. Uji-i, *Angewandte Chemie International Edition* **59**, 5332 (2020).
- [8] F. J. Garcia-Vidal, C. Ciuti, and T. W. Ebbesen, *Science* **373**, eabd0336 (2021).
- [9] A. Thomas, L. Lethuillier-Karl, K. Nagarajan, R. M. A. Vergauwe, J. George, T. Chervy, A. Shalabney, E. Devaux, C. Genet, J. Moran, and T. W. Ebbesen, *Science* **363**, 615 (2019).
- [10] J. Lather and J. George, *The Journal of Physical Chemistry Letters* **12**, 379 (2021).
- [11] J. Lather, A. N. K. Thabassum, J. Singh, and J. George, *Chemical Science* **13**, 195 (2022).
- [12] W. Ahn, F. Herrera, and B. Simpkins, *Modification of Urethane Addition Reaction via Vibrational Strong Coupling* (2022).
- [13] A. D. Dunkelberger, B. T. Spann, K. P. Fears, B. S. Simpkins, and J. C. Owrutsky, *Nature Communications* **7**, 13504 (2016).
- [14] B. Xiang, R. F. Ribeiro, A. D. Dunkelberger, J. Wang, Y. Li, B. S. Simpkins, J. C. Owrutsky, J. Yuen-Zhou, and W. Xiong, *Proceedings of the National Academy of Sciences* **115**, 4845 (2018).
- [15] B. Xiang, R. F. Ribeiro, M. Du, L. Chen, Z. Yang, J. Wang, J. Yuen-Zhou, and W. Xiong, *Science* **368**, 665 (2020).
- [16] Y. Pang, A. Thomas, K. Nagarajan, R. M. A. Vergauwe, K. Joseph, B. Patrahaui, K. Wang, C. Genet, and T. W. Ebbesen, *Angewandte Chemie International Edition* **59**, 10436 (2020).
- [17] J. Yuen-Zhou, J. A. Campos-González-Angulo, R. F. Ribeiro, and M. Du, in *Metamaterials, Metadevices, and Metasystems 2021*, Vol. 11795, edited by N. Engheta, M. A. Noginov, and N. I. Zheludev, International Society for Optics and Photonics (SPIE, 2021) p. 117950K.
- [18] B. Peters, *Reaction rate theory and rare events* (Elsevier, 2017).
- [19] J. Galego, C. Climent, F. J. Garcia-Vidal, and J. Feist, *Physical Review X* **9**, 021057 (2019).
- [20] X. Li, A. Mandal, and P. Huo, *Nature Communications* **12**, 1315 (2021).
- [21] P.-Y. Yang and J. Cao, *The Journal of Physical Chemistry Letters* **12**, 9531 (2021).
- [22] R. F. Grote and J. T. Hynes, *The Journal of Chemical Physics* **73**, 2715 (1980).
- [23] F. J. Hernández and F. Herrera, *The Journal of Chemical Physics* **151**, 144116 (2019).
- [24] J. F. Triana, F. J. Hernández, and F. Herrera, *The Journal of Chemical Physics* **152**, 234111 (2020).
- [25] J. A. Campos-Gonzalez-Angulo, R. F. Ribeiro, and J. Yuen-Zhou, *New Journal of Physics* **23**, 063081 (2021).
- [26] R. F. Ribeiro, A. D. Dunkelberger, B. Xiang, W. Xiong, B. S. Simpkins, J. C. Owrutsky, and J. Yuen-Zhou, *The Journal of Physical Chemistry Letters* **9**, 3766 (2018).
- [27] N. M. Hoffmann, L. Lacombe, A. Rubio, and N. T. Maitra, *The Journal of Chemical Physics* **153**, 104103 (2020).
- [28] R. F. Ribeiro, *Communications Chemistry* **5**, 1 (2022).
- [29] C. Schäfer, J. Flick, E. Ronca, P. Narang, and A. Rubio, arXiv preprint arXiv:2104.12429 (2021).
- [30] D. S. Wang, T. Neuman, S. F. Yelin, and J. Flick, *The Journal of Physical Chemistry Letters* **13**, 3317 (2022).
- [31] D. S. Wang, J. Flick, and S. F. Yelin, *Chemical reactivity under collective vibrational strong coupling* (2022).
- [32] E. W. Fischer, J. Anders, and P. Saalfrank, *The Journal of Chemical Physics* **156**, 154305 (2022).
- [33] D. Sidler, C. Schäfer, M. Ruggenthaler, and A. Rubio, *The Journal of Physical Chemistry Letters* **12**, 508 (2021).
- [34] T. Botzung, D. Hagenmüller, S. Schütz, J. Dubail, G. Pupillo, and J. Schachenmayer, *Physical Review B* **102**, 144202 (2020).
- [35] J. A. Campos-Gonzalez-Angulo, Y. R. Poh, M. Du, and J. Yuen-Zhou, *Swinging between shine and shadow: Theoretical advances on thermally-activated vibropolaritonic chemistry (a perspective)* (2022).
- [36] J. A. Campos-Gonzalez-Angulo, R. F. Ribeiro, and J. Yuen-Zhou, *Nature Communications* **10**, 4685 (2019).
- [37] I. Vurgaftman, B. S. Simpkins, A. D. Dunkelberger, and J. C. Owrutsky, *The Journal of Physical Chemistry Letters* **11**, 3557 (2020).

- [38] N. T. Phuc, P. Q. Trung, and A. Ishizaki, *Scientific Reports* **10**, 7318 (2020).
- [39] M. Du, J. A. Campos-Gonzalez-Angulo, and J. Yuen-Zhou, *The Journal of Chemical Physics* **154**, 084108 (2021).
- [40] M. Du and J. Yuen-Zhou, *Physical Review Letters* **128**, 096001 (2022).
- [41] Y. R. Poh, S. Pannir-Sivajothi, and J. Yuen-Zhou, *Understanding the Energy Gap Law under Vibrational Strong Coupling* (2022).
- [42] J. Cao, *The Journal of Physical Chemistry Letters* **13**, 10943 (2022).
- [43] J. Sun and O. Vendrell, *The Journal of Physical Chemistry Letters* **13**, 4441 (2022).
- [44] L. P. Lindoy, A. Mandal, and D. R. Reichman, *The Journal of Physical Chemistry Letters* **13**, 6580 (2022).
- [45] J. P. Philbin, Y. Wang, P. Narang, and W. Dou, *The Journal of Physical Chemistry C* **126**, 14908 (2022).
- [46] E. Pollak, H. Grabert, and P. Hänggi, *The Journal of Chemical Physics* **91**, 4073 (1989).
- [47] H. A. Kramers, *Physica* **7**, 284 (1940).
- [48] V. I. Mel'nikov and S. V. Meshkov, *The Journal of Chemical Physics* **85**, 1018 (1986).
- [49] E. Pollak, *The Journal of Chemical Physics* **85**, 865 (1986).
- [50] J. del Pino, J. Feist, and F. J. Garcia-Vidal, *The Journal of Physical Chemistry C* **119**, 29132 (2015).
- [51] K. S. Daskalakis, S. A. Maier, and S. Kéna-Cohen, in *Quantum Plasmonics*, Springer Series in Solid-State Sciences, Vol. 185, edited by S. I. Bozhevolnyi, L. Martin-Moreno, and F. Garcia-Vidal (Springer, 2017) Chap. 7, pp. 151–163.
- [52] K. S. U. Kansanen, *Theory for polaritonic quantum tunneling* (2022).
- [53] J. Flick, M. Ruggenthaler, H. Appel, and A. Rubio, *Proceedings of the National Academy of Sciences* **114**, 3026 (2017).
- [54] V. Rokaj, D. M. Welakuh, M. Ruggenthaler, and A. Rubio, *Journal of Physics B: Atomic, Molecular and Optical Physics* **51**, 034005 (2018).
- [55] C. Schäfer, M. Ruggenthaler, V. Rokaj, and A. Rubio, *ACS Photonics* **7**, 975 (2020).
- [56] G. D. Wiesehan and W. Xiong, *The Journal of Chemical Physics* **155**, 241103 (2021).
- [57] D. P. O'Leary and G. W. Stewart, *Journal of Computational Physics* **90**, 497 (1990).
- [58] R. Chikkaraddy, B. de Nijs, F. Benz, S. J. Barrow, O. A. Scherman, E. Rosta, A. Demetriadou, P. Fox, O. Hess, and J. J. Baumberg, *Nature* **535**, 127 (2016).
- [59] O. Bitton and G. Haran, *Accounts of Chemical Research* **55**, 1659 (2022).
- [60] J. del Pino, J. Feist, and F. J. Garcia-Vidal, *New Journal of Physics* **17**, 053040 (2015).
- [61] M. Du, L. A. Martínez-Martínez, R. F. Ribeiro, Z. Hu, V. M. Menon, and J. Yuen-Zhou, *Chemical Science* **9**, 6659 (2018).